

NC1.2 FREE CONVECTIVE HEAT TRANSFER IN THE SUPERCRITICAL REGION

E. Hahne, G. Feurstein and U. Grigull

Institut A für Thermodynamik, Technische Universität München, Germany

Abstract

Experiments were performed under pool conditions on horizontal wires in two different pressure vessels filled with supercritical carbon dioxide. The pressure ratio ranged from $p_b/p_c = 1.002 \div 1.29$, the temperature ratio $t_b/t_c = 0.322 \div 1.77$. Platinum and nickel-chromium alloy wires were used. Enhancement in heat transfer, with peaks in the heat transfer coefficients, strongly depends on the relation of bulk- and film-temperature to the pseudo-critical temperature. The formation of bubble-like structures on various nichrome wires was observed in either vessel.

NOMENCLATURE

c_p : Specific heat, kJ/kg K
 C : Constant
 d : Diameter, mm
 h : Heat transfer coefficient, W/cm²K
 k : Thermal conductivity, W/m K
 l : Length, mm
 n : Exponent
 t : Temperature, °C
 p : Pressure, bar
 q : Heat flux, W/cm²
 Nu : Nusselt-number
 Pr : Prandtl-number
 Ra : Rayleigh-number
 β : Coefficient of thermal expansion, 1/K
 ν : Kinematic viscosity, m²/s
 ρ : Density, kg/m³

Subscripts

b : Bulk
 c : Critical
 F : Film
 pc : Pseudo-critical
 w : Wire

1. INTRODUCTION

Application of high pressures and temperatures in modern power plants, transport problems with cryogenic fluids in rockets or utilization of superconductivity effects, revived interest in heat transfer phenomena in the thermodynamic supercritical region.

An excellent survey of research in this field, done in many countries until 1970, is given by Hendricks et al. [1]. For brevity only this reference shall be quoted here for the many papers considered in this work.

Here, two main points of dispute for the enhancement of heat transfer are given extensive experimental investigation: influence of the thermodynamic state and boiling-like action. Experiments were performed in a free convection pool arrangement thus providing high accuracy in control of temperatures of both the critical fluid and the heating element, and avoiding pressure and velocity fluctuations induced from outside. Possible influences of Pressure vessel

geometry could be observed by using two different pressure vessels, a cylindrical one (c) described in [2] and a rectangular one (r) described in [3]. For heating elements, horizontal wires of lengths 70 mm (c) (= used in the cylindrical vessel) and 100 mm (r), and of different diameters 0,05; 0,1; 0,25 and 0,3 mm were used. The wire material was either platinum or Ni-Cr-alloys; the test fluid was carbon dioxide.

With fluid pressures of 74, 75, 80, 85, 90, 95 bar a pressure range of $p_b/p_c = 1.002 \div 1.287$ is covered and with bulk fluid temperatures of 10; 20; 25; 28; 30,5; 31; 32; 55 °C a temperature ratio of $t_b/t_c = 0.322 \div 1.771$. Temperature differences between the heated wire and the bulk fluid came up to 900 K.

2. EXPERIMENTAL PROCEDURE

The experiments were performed at constant pressure and constant bulk temperature. The pressure was kept constant by using charge vessels connected to the test vessels but heated separately. Fluid bulk temperatures were preserved by submerging the vessel (c) into a thermostatically controlled bath or by having thermostat water running through tubes surrounding the pressure vessel (r) with good thermal contact. The electric input to the wire was altered in steps, thus changing the wire temperature and the driving temperature difference. For power supply a high accuracy AC-transformer was used. Wire temperatures were determined from the voltage drop across the wire and a calibrated normal resistance, thus the wire was made a resistance thermometer. Fluid bulk temperatures were obtained from two thermocouples within the pressure vessels. All electric data were registered on a HP-digital voltmeter and processed on a data acquisition system. Pressures were read from Heise-gauges.

3. THERMOPHYSICAL PROPERTIES

For any state, thermophysical properties were recalled from computer programs. Density ρ , specific heat $c_p = (\partial h / \partial T)_p$ and the coefficient of thermal expansion $\beta = (-1/\rho)(\partial \rho / \partial T)_p$ were derived from an equation of state given

in [4] and compared to other equations [5]. Data for thermal conductivity k and the dynamic viscosity ν are based on equations given in [6].

For pressures applied in these experiments the respective pseudocritical temperatures, ratios of critical to pseudo-critical pressures and temperatures are given in table 1.

$p = p_{pc}$	74	75	80	85	90	95	bar
t_{pc}	31,2	31,7	34,6	37,3	39,9	42,3	$^{\circ}\text{C}$
p_c/p_{pc}	0,9978	0,9845	0,9229	0,8686	0,8204	0,7772	-
t_c/t_{pc}	0,9955	0,9798	0,8977	0,8327	0,7785	0,7343	-

TABLE 1

For the critical state of CO_2 , $p_c = 73.84$ bar, $t_c = 31.06$ $^{\circ}\text{C}$. For a given supercritical pressure, the respective pseudo-critical temperature is defined as that temperature where the specific heat reaches a maximum. (In literature also "transposed critical temperature" is used). It is worthy to note from table 1 that an approximation is valid for pressures up to 80 bar: $p_c/p_{pc} \approx t_c/t_{pc}$.

4. RESULTS AND DISCUSSION

4.1.1. Platinum wires in the rectangular vessel.

For a constant pressure of 74 bar and a variety of 6 bulk fluid temperatures, the heat flux from a platinum wire, 100 mm long and 0.1 mm in diameter, is given in figure 1 as a function of wire temperature.

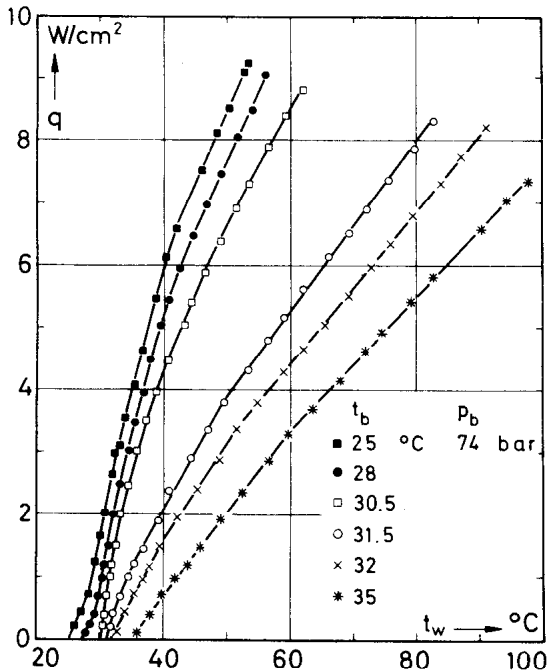


Fig. 1: Heat flux q vs. wire temperature t_w for various bulk temperatures at constant bulk pressure.

Two sets of curves differing distinctly in dq/dt_w are obvious. For bulk fluid temperatures $t_b = 25; 28; 30.5$ $^{\circ}\text{C}$, which are smaller than the pseudo-critical temperature of $t_{pc} = 31.2$ $^{\circ}\text{C}$, pertinent to the pressure of 74 bar (table 1), the increase dq/dt_w is considerably larger than in those cases where the bulk fluid temperature

exceeds the pseudo-critical temperature, for $t_b = 31.5; 32; 35$ $^{\circ}\text{C}$. With the heat transfer coefficient $h \sim dq/dt_w$, consequently the heat transfer is larger for conditions $t_b < t_{pc}$ than for $t_b > t_{pc}$, and the S-shape of curves for $t_b < t_{pc}$ indicates a maximum in h .

In figure 2 these results are presented with heat transfer coefficient vs. wire temperature corresponding to the parameters of figure 1.

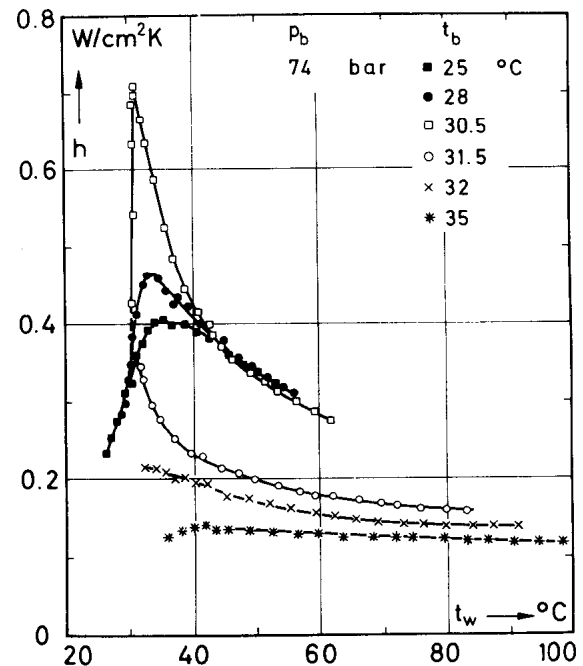


Fig. 2: Heat transfer coefficient h vs. wire temperature t_w for various bulk temperatures at constant bulk pressure.

Distinct peaks are obtained only for bulk fluid conditions below the pseudo-critical, i. e. with a given pressure $p_b = p_{pc} = 74$ bar for temperatures $t_b < t_{pc} = 31.2$ $^{\circ}\text{C}$. The closer the bulk temperature is to the pseudo-critical the more pronounced are these peaks. For bulk temperatures exceeding the respective pseudo-critical only a

little, $t_b \gtrsim t_{pc}$, the heat transfer coefficient drops off remarkably in a way as if an h -peak value has just been exceeded. A characteristic curve is given for a fluid temperature of $t_b = 31.5 \text{ }^\circ\text{C}$. At a temperature ratio $t_b/t_{bc} = 1.12$, for $t_b = 35 \text{ }^\circ\text{C}$, the heat transfer coefficient remains almost constant at a value of about 15% of the largest peak value. A small hump is observed for heat transfer coefficients connected to small temperature differences.

Such a behaviour is characteristic for other bulk pressures as well, and the formation of peaks is not restricted to bulk temperatures below the critical temperature, as might be concluded from figure 2.

In figure 3 the heat transfer coefficient is presented for a constant supercritical bulk temperature $t_b = 31.5 \text{ }^\circ\text{C}$ and a variety of six pressures. The pseudo-critical pressure corresponding to $t_b = t_{pc} = 31.5 \text{ }^\circ\text{C}$ is around 74.8 bar.

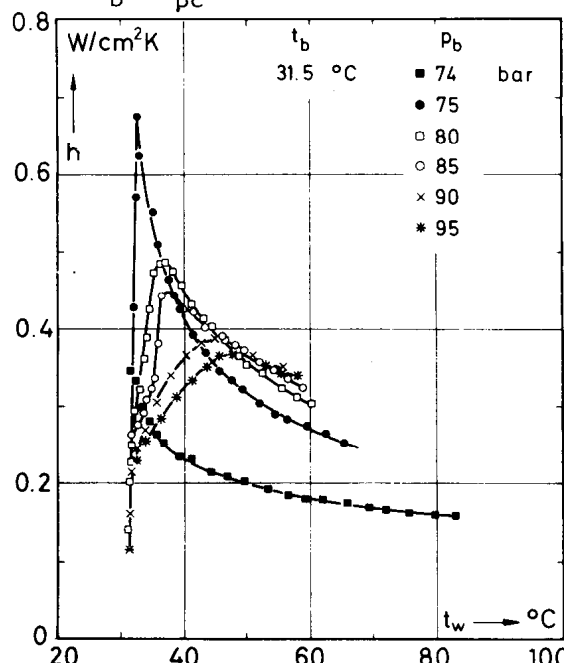


Fig.3: Heat transfer coefficient h vs. wire temperature t_w for various bulk pressures at supercritical bulk temperature.

For the thermodynamic state of the CO_2 in the vessel, this means that pseudo-critical conditions are already exceeded for $t_b = 31.5 \text{ }^\circ\text{C}$ and $P_b = 74 \text{ bar}$, they are not yet reached, however, for bulk pressures $P_b \gtrsim 75 \text{ bar}$. Consequently the heat transfer coefficient decreases to low values for $P_b = 74 \text{ bar}$ while peaks form for all other pressures applied.

4.1.2 Platinum wires in the cylindric vessel

These experiments were performed with wires 70 mm long and 0.05 mm or 0.3 mm in diameter. Temperature differences, $t_w - t_b$, up to 900 K were applied. For this reason, the temperature difference is plotted on a logarithmic abscissa

scale in figure 4. In this diagram the heat transfer coefficient on a 0.3 mm wire is plotted for a constant bulk pressure $P_b = 85 \text{ bar}$ and six different bulk temperatures. In all characteristics the curves are alike those described for the rectangular pressure vessel, so that pressure vessel influences as causes of heat transfer peculiarities can be excluded.

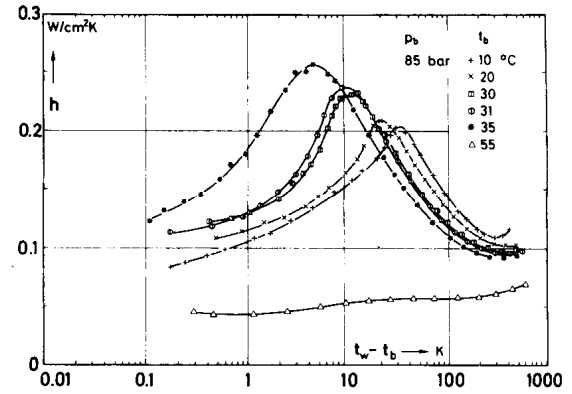


Fig.4: Heat transfer coefficient h vs. temperature difference $t_b - t_w$ for various bulk temperatures at constant bulk pressure (cylindric pressure vessel, platinum wire: $d = 0.3 \text{ mm}$, $l = 70 \text{ mm}$).

The favourable heat transfer conditions encountered when the bulk fluid temperature is below the pseudo-critical are maintained -although less pronounced- up to temperature differences of about 900 K. Thus, for technical use, it is advantageous in any case, to span the pseudo-critical temperature between heating element and fluid temperature.

It is also observed from figure 4 that the enhancement of heat transfer coefficients is not restricted to only very small temperature differences. For a bulk temperature $t_b = 10 \text{ }^\circ\text{C}$ e.g. a peak, amounting to a 100% increase in heat transfer coefficient, is found for a temperature difference of 33 K. Comparing figure 4 to 2 it is observed that peak values of h are larger for bulk conditions closer to the critical point. Thus, both an influence of critical and pseudo-critical temperature appears inherent in heat transfer in the supercritical region.

4.2 Nickel-chromium-alloy wires

These experiments were performed in both the rectangular and the cylindric pressure vessel. U.S. nichrome wires No. V and VII, with a diameter of 0.254 mm (0.01 inch) and German Chronitherm-wires (diameter 0.25 mm) were used. In figure 5 a comparison of heat flux is presented for nichrome VII (0.254 mm) and platinum wires of 0.05 and 0.3 mm diameter, each 70 mm long and at constant bulk conditions $P_b = 85 \text{ bar}$, $t_b = 31 \text{ }^\circ\text{C}$. A deviation of the nichrome wire data is obvious. This deviation is due to special phenomena such as wire oscillation and

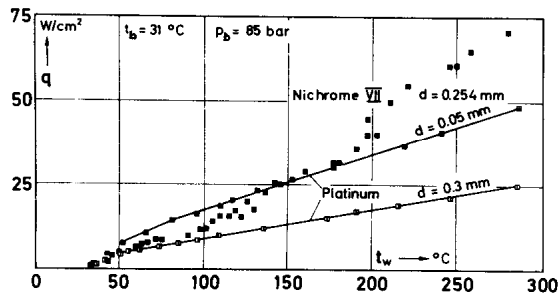


Fig. 5: Comparison of heat flux q vs. wire temperature for platinum and nichrome VII wires, at constant bulk temperature and pressure (cylindric pressure vessel, wire lengths: $l = 70$ mm).

formation of bubble-like structures. These phenomena are described in detail in [2], [7].

In figure 5, the unusual increase of nichrome wire heat flux for wire temperatures beyond $t_w = 100$ °C results from the onset of oscillations of the wire and successive formation of bubble-shaped structures on the lower side of the wire. While observable oscillations ceased at around $t_w = 150$ °C, the formation of bubble structures continued up to $t_w = 300$ °C. These bubbles were best visible when bulk pressure was high and bulk temperature low ($t_b < t_{pc}$), but they also appeared with bulk conditions exceeding the pseudo-critical state for both nichrome and chronitherm wires. Test runs for thermodynamic conditions as given in [2] yielded perfect agreement to those results. On a platinum wire, under exactly the same experimental conditions no such phenomena were observed. This suggested the assumption that the phenomena are material specific. Investigation in this respect revealed the following differences:

Observation of fluid flow around platinum and nichrome wires showed that the turbulent buoyancy plume never adheres to the platinum wire but sticks to the nichrome wire when a certain heat flux is reached.

For platinum, the flow around the wire appears laminar and becomes turbulent some distance above the wire. This principal pattern remains up to wire temperatures $t_w = 900$ °C. For nickel-chromium alloys the laminar circumflow ceases with the onset of wire oscillation when the turbulent plume periodically comes to a touch with the wire at around $t_w = 100$ °C. When the turbulent zone permanently adheres to the wire, at $t_w = 150$ °C, the oscillations cease.

Surface finish of platinum and nichrome wires were compared in a Raster-Electron microscope, at a 2000 times magnification. Platinum is the softer material and its surface appears relatively smooth compared to nichrome with craters and cracks forming a rough surface. A test run

with an artificially roughened (sand-papered) platinum wire did not bring extraordinary results comparable to nichrome. A test run with half the chronitherm wire annealed and oxidized while the other half remained blank, did not bring differences in flow patterns.

The temperature coefficient of electrical resistance for platinum is about 15 times as large as that for nichrome. Moreover, the temperature dependence of the electrical resistance of nichrome does substantially deviate from the linear at temperatures exceeding 350 °C. Repeated calibrations of the nichrome wires produced ageing and hysteresis effects amounting to 8% deviations.

More detailed research on possible high frequency oscillations of the wire or on chemical reaction of nichrome components is performed.

5. CORRELATIONS

A Nusselt type correlation of the simple kind $Nu = C Ra^n$ is given in figure 6 for 0.3 mm platinum wire data at a bulk pressure of $p_b = 75$ bar. All properties are taken at film temperature $t_f = (t_b + t_w)/2$. Radiative heat transmission is neglected.

Roughly three different curves can be related to the data: a branch **I**, correlating the data for bulk and film temperatures smaller than the pseudo-critical temperature; a branch **II** for the case where the bulk temperature is still below the pseudo-critical but with film temperature exceeding it and a branch **III** for data obtained when both bulk and film temperature exceed the pseudo-critical temperature. Curve **I** characterizes increasing Nu with increasing Ra , while **II** gives decreasing Nu with decreasing Ra . For curve **III**, at $t_b = 35$ °C, Nusselt-number values fall on one line for both increasing and decreasing Rayleigh-numbers; for $t_b = 55$ °C, however, this does not hold. These data representing a thermodynamic state in the pressure vessel, somewhat removed from the near pseudo-critical seem to approach curve **I**. Scatter in correlation data is very large for the highest Rayleigh-numbers coinciding with the pseudo-critical state. Principally the same characteristic curves are obtained for other bulk pressures. For higher bulk pressures the scatter in correlation data is less.

6. CONCLUSIONS

6.1 Identical experiments performed in two pressure vessels of different geometry prove no major influence of geometry on heat transfer peculiarities in the near critical region.

6.2 Results for heat transfer coefficients reveal a decisive importance of pseudo-critical

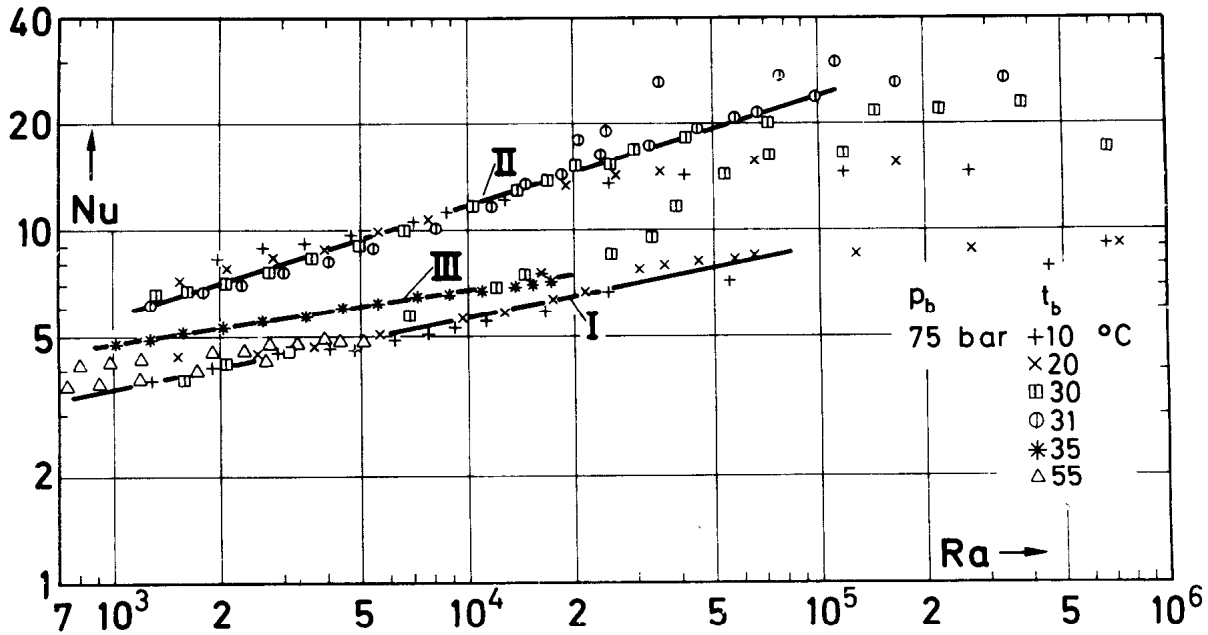


Fig. 6: Correlation of Nusselt-number vs. Rayleigh-number for various bulk temperatures at constant bulk pressure (cylindric pressure vessel, platinum wire: $d = 0.3 \text{ mm}$, $l = 70 \text{ mm}$).

states for heat transfer in the supercritical region. Roughly three different tendencies are discerned, depending on bulk-, film- and pseudo-critical temperatures at a given pressure:

an increasing heat transfer coefficient for:

$$t_b, t_F < t_{pc}$$

a decreasing heat transfer coefficient for:

$$t_b < t_{pc} < t_F$$

a decreasing or an almost constant heat transfer coefficient for: $t_b, t_F > t_{pc}$.

6.3 Different location and inclination of curves in a Nusselt type correlation suggest a subdivision of correlation equations specific to each temperature region listed in 6.2.

6.4 Identical experiments performed with platinum and nichrome wires proved heat transfer phenomena encountered with nichrome wires to be material specific.

ACKNOWLEDGMENT

The authors want to express their gratitude to Professor R. H. Sabersky for providing the cylindric pressure vessel and the nichrome wires. All calculations on properties were performed on the TR 440 of the Technical University of Munich. Disposition of calculation time is gratefully acknowledged.

REFERENCES

[1] Hendricks, R. C., R. J. Simeoneau and R. V. Smith: "Survey of Heat Transfer of near Critical Fluids, NASA TN D-5886, November 1970.

- [2] Knapp, K. K. and R. H. Sabersky: "Free Convection Heat Transfer to Carbon Dioxide near the Critical Point" *Int. Journ. Heat Mass Transfer* 9, 41 (1966)
- [3] Abadzic, E.: "Wärmeübergang beim Sieden in der Nähe des kritischen Punktes", D. Eng. Thesis, Technische Hochschule München (1967)
- [4] Meyer-Pittroff, R.: "Die Aufstellung einer kanonischen Zustandsgleichung für Kohlendioxid durch Approximation verschiedenartiger Vorgabewerte", D. Eng. Thesis, Technische Universität München (1973)
- [5] Bender, E.: "Equations of State Exactly Representing the Phase Behaviour of Pure Substances". *Proc. Fifth Symp. Thermophys. Prop.*, Newton, Mass. (1970), p. 227
- [6] Wukalowitsch, M. P. and V. V. Altunin: "Thermophysical Properties of Carbon Dioxide", London/Wellingborough (1968)
- [7] Nishikawa, K., T. Ito and H. Yamashita: "Free Convective Heat Transfer to a Supercritical Fluid", *Memoirs of the Faculty of Engineering, Kyushu University*, Vol. XXX, No. 2 (1970).